Silver nanoparticle-adjuvanted vaccine protects against lethal influenza infection through inducing BALT and IgA-mediated mucosal immunity

Daniel Sanchez-Guzman, Pierre Le Guen, Berengere Villeret, Nuria Sola, Remi Le Borgne, Alice Guyard, Alix Kemmel, Bruno Crestani, Jean-Michel Sallenave, Ignacio Garcia-Verdugo

Silver nanoparticle-adjuvanted vaccine protects against lethal Influenza infection through inducing BALT and IgA-mediated mucosal immunity

Daniel Sanchez-Guzman[1,†], Pierre Le Guen[1,2,†], Berengere Villeret[1], Nuria Sola[1], Remi Le Borgne[3], Alice Guyard[4], Alix Kemmel[1], Bruno Crestani[1,2], Jean-Michel Sallenave[1], Ignacio Garcia-Verdugo[1*]

1. INSERM, UMR U1152, Laboratoire d'Excellence Inflamex, Département Hospitalo-Universitaire FIRE (Fibrosis, Inflammation and Remodeling), Université Paris Diderot, Sorbonne Paris Cité, 75018 Paris, France.

2. Department of Pneumology A, AP-HP, Groupe Hospitalier Bichat-Claude Bernard, Paris, 75018 Paris, France.

3. ImagoSeine, Electron Microscopy Facility, Institut Jacques Monod, CNRS UMR 7592, Université Paris Diderot, Sorbonne Paris Cité, 75205 Cedex 13 Paris, France.

4. Department of Pathology, AP-HP, Groupe Hospitalier Bichat-Claude Bernard, Paris, 75018 Paris, France.

† Equal contribution.

Declarations of interest: none

* To whom correspondence should be addressed: ignacio.garcia-verdugo@inserm.fr

Inserm UMR1152, Physiopathologie et Epidémiologie des Maladies Respiratoires, Université Paris 7 Diderot, Faculté de Médecine, site Bichât, 16, rue Henri Huchard 75018 Paris, FRANCE.

Tel: +33157277801. Fax: +33157277551.

Abstract

Most of current influenza virus vaccines fail to develop a strong immunity at lung mucosae (site of viral entry) due to sub-optimal vaccination protocols (*e.g.* inactivated virus administered by parenteral injections). Mucosal immunity could be improved by using locally-delivered vaccines containing appropriate adjuvants. Here we show, in a mouse model, that inclusion of silver nanoparticles (AgNPs) in virus-inactivated flu vaccine resulted in reduction of viral loads and prevention of excessive lung inflammation following influenza infection. Concomitantly, AgNPs enhanced specific IgA secreting plasma cells and antibodies titers, a hallmark of successful mucosal immunity. Moreover, vaccination in the presence of AgNPs but not with gold nanoparticles, protected mice from lethal flu. Compared with other commercial adjuvants (squalene/oil-based emulsion) or silver salts, AgNPs stimulated stronger antigen specific IgA production with lower toxicity by promoting bronchus-associated lymphoid tissue (BALT) neogenesis, and acted as a *bona fide* mucosal adjuvant.

Keywords: silver nanoparticles, influenza virus, vaccine, adjuvant, lung vaccination, immunity

Introduction

The main goal of prophylactic vaccination against flu is to induce protective immunity at the respiratory tract (the port of entry of the influenza virus), but current protocols are still by large inadequate. Most of the current influenza vaccines consist of inactivated virus that is administered by parenteral injection. Unfortunately, these conditions of administration (inactivated virus and systemic route) do not favour the induction of a robust immune mucosal response*[1,2]*, contrary to live attenuated influenza vaccines administered by the pulmonary route*[3]*. The latter promotes more efficiently local specific immunity specially in children but is less efficient in elderly people and also presents obvious safety limitations*[4]* . Therefore, an ideal mucosal anti-Influenza vaccine should consist of a 'safe particle' (ideally inactivated and not attenuated), which in conjunction with an appropriate adjuvant should nevertheless be able to break the tolerogenic environment associated with mucosa[5–7]. Ideally, it should also down-regulate unwanted inflammatory 'sequelae' sometimes derived from Influenza infections, particularly when associated with pandemic strains. Indeed, Influenza, alone, or in combinations with further microbial infections (often of bacterial origin) can induce fatal pneumoniae, through the well-recognized 'cytokine storm'*[8]*. Independently of their underlying molecular mechanism of action, most of adjuvants induce a transient local inflammation illustrated by the expression of pro-inflammatory cytokines and chemokines (IL-12, IL-6, CCL-2, CXCL-1, CCL-5) and a rapid infiltration and activation of innate immune cells (neutrophils, monocytes, DC) at the site of administration*[9,10]*. These 'innate-immune events' help to prime T and B cells in local lymph nodes (LN) resulting into higher antibody and cellular responses to the vaccine antigens. For instance, MF59 a squalene-based oil-in water emulsion adjuvant has been licensed and included in adjuvanted flu vaccines administered parenterally demonstrating encouraging

vaccination outcomes*[11]*. These preparations seem to be acting through mechanisms that are still not fully understood*[9]* , but seemingly independently of Toll-like receptors (TLRs), and through 'carrier/depot' effects, which increase and lengthens the accumulation of the antigen at mucosal sites.

Similarly, nanomaterials have recently been included in vaccine formulations to improve their efficacy and effectiveness*[12]* . For instance, biodegradable-polymer based nanoparticles (NP) have been used as carriers in flu vaccines demonstrating an increased depot effect of the antigen associated to prolonged and sustained higher antibody titers[13–15]. Interestingly, metallic NPs, and particularly silver (Ag) nanoparticles (AgNPs) have been shown to modulate innate immunity*[16]* , promoting the release of pro-inflammatory cytokines *in vitro* in innate immune cells[17–19] and *in vivo* after pulmonary administration in rodents*[20,21]* . Moreover, synthetic NPs present high surface energies (due to their high surface area ratio), which in complex media drives spontaneous adsorption of proteins to the NP surface, constituting the so called 'protein corona'. This property of NPs has been exploited to enhance antigen transport and distribution in vaccine applications[22,23].

Here departing from previously used parenteral protocols, we show that AgNPs are a potent adjuvant when administered intra-peritoneally, and more significantly in the lung during pulmonary immunisation. We demonstrate a physical interaction between AgNPs and antigen, favouring micro-depots, which in turns promotes bronchus-associated lymphoid tissue (BALT) generation. This induces IgA-mediated mucosal immunity which protects mice against Influenza infection more efficiently than other alternative adjuvants, *e.g.* polyIC (a TLR-3 ligand), and AddaVax (a MF59 like-adjuvant used in experimental protocols). Crucially, we also demonstrate that AgNPs are instrumental in down-regulating concomitant Influenza-mediated lung inflammation.

Materials and Methods

Cell culture. All cell culture reagents were from Invitrogen unless stated. The MPI alveolar macrophage cell line [gift from Dr. G. Feje] [24] was cultured at 37°C in a 5% CO_2 in RPMI medium containing 10% FCS, Glutamax, penicillin (100U/ml), streptomycin (100µg/ml) and 30 ng/mL of mGM-CSF (PeproTech). Bone marrow derived dendritic cells (BMDC) were obtained as described before*[25]*. Briefly, cells from the bone marrow of the femurs of C57Bl/6 mice were seeded at $4x10^5$ cells/mL in the same medium described above but supplemented with β-Mercaptoethanol (50nM) and mGM-CSF (30ng/mL). On days 3, 6 and 8 the medium was refreshed and mGM-CSF was added. At day 10, non-adherent cells were harvested. MPI and BMDC were stimulated in the corresponding media with LPS (100ng/ml) from *P.aeruginosa* (Sigma, L-8643) or AgNPs (2.5-10 µg/mL) for 24h and then cytokines were measured in the supernatants.

Influenza virus. Influenza virus strain A/Scotland/20/74 (H3N2) (abbreviated as IAV) was a gift from Professor van der Werf (Pasteur Institute, Paris). Virus was routinely amplified in MDCK cells (ATCC CCL-34) as described before*[26,27]*. From the supernatants of infected cells, influenza virus was purified by centrifugation in sucrose gradient, aliquoted and kept at -80°C until use. Plaque forming units (PFU/ml) of influenza stocks were quantified by the virus plaque assay*[27]* (see below). When needed, purified samples were inactivated by heating at 95°C for 10min in a block heater. Inability of heat-inactivated influenza virus (IAV*) to replicate was then confirmed by the virus plaque assay.

Virus plaque assay. MDCK cells were grown until confluency in p6 well plates in MEM medium containing glutamine, antibiotics and 5% FCS. Then, 1/10 serial dilutions of either influenza stocks or lung homogenates from infected mice were added to the cells and incubated for 1h at 37°C in a humidified incubator. TPCK-trypsin (Worthington) (1µg/ml final concentration) and Avicel microcrystalline cellulose (1.2 % w/v) (FMC Biopolymer) were then added and infected monolayers were incubated for 48h. After washing, cell monolayers were stained with crystal violet and lysis plaques (pfu) were counted and referred to the volume of the influenza stock solution or lung homogenate.

Endotoxin assessment in nanoparticle solutions. Endotoxin content in AgNPs stocks was measured by the LAL Chromogenic Endotoxin Quantitation kit (Pierce) following the manufacturer's instructions and using doses of AgNPs that did not interfere with the assay as described before*[28]*. Interference of AgNPs with the assay was measured by including AgNPs in the standard curve and comparing OD_{405nm} of the LPS standard with or without AgNPs. Possible interferences due to yellowish colour of AgNPs in solution was controlled by measuring OD_{405nm} in tubes where AgNPs were added after the stop reagent.

Influenza infection and vaccination procedures. Animal experiments were performed according to the European Union guidelines for the handling of laboratory animals. Our protocol was approved by the National Ethics Committee (CE No.121) and the French Ministry of Education and Research (agreement No. 02012).

Influenza infection. C57Bl/6J mice were purchased from Janvier Laboratories (L'Arbresle, France). Mice were anesthetized with a mixture of ketamine–xylazine, administered

intraperitoneally, and were then intranasally instilled with 40µl of PBS alone or with 40µl of PBS containing 300 or 1000 plaque-forming units (pfu) of influenza virus as described before*[26]* .

Intraperitoneal vaccination. Seven-week-old C57Bl/6 male mice were primed with 50µg of KLH (Sigma) combined either with vehicle (PBS/2mM citrate buffer), with 50µg of AgNPs or with 50µg of polyinosinic–polycytidylic acid (Poly IC) (Sigma) (total volume 100µl) administered by the intraperitoneal route. 8 days later, a boost consisted in administration of half-dosage of the same antigen/adjuvant combination used in priming. 8 days after the boost, blood was collected and mice culled to perform peritoneal lavages (10ml) (PLs) and to collect spleens. Serum was extracted from blood samples for titration of antibodies. Cytokines and cellular populations in PLs were identified by ELISA and flow cytometry, respectively. Peripheral blood mononuclear cells (PBMC) from spleen homogenates were obtained by differential centrifugation in Lympholyte-M (Cedarlane) and were used to detect plasma cells by ELISPOT. In other set of experiments, mice were treated with AgNPs (50µg) injected intraperitoneally in 100µL and 4h later PLs were performed to measure cellular recruitment (flow cytometry) and cytokines (ELISA).

Pulmonary vaccination. Antigen (KLH or IAV*) was combined to either vehicle (PBS/2mM citrate buffer), AgNPs (25µg), Poly IC (25µg), AddaVax (10µL) (InvivoGen), AuNPs (25µg) or $AgNO_3$ (25µg, Sigma). Seven-week-old C57Bl/6 male mice were anesthetized as described above and primed with either KLH (50µg) or heat-inactivated influenza virus (IAV*) (12µg of total protein) administered intratracheally in 50µl (final volume), with or without adjuvants (see above). 10 days later, a boost consisted in half-dose of the same antigen/adjuvant combination used in priming, except for $AgNO_3$ which was used at 25% of the initial dose (6.5 µg) to reduce toxicity (Fig-S3). 10 days after the boost, blood was collected and mice culled to perform

bronchoalveolar lavages (BALs) with PBS (2ml) and collect paratracheal lymph nodes and lungs (previously perfused with 0.9% NaCl through the pulmonary artery). In another set of experiments, mice were treated only with AgNPs administered intratracheally. At days 1, 3 and 6 after instillation, mice were culled and BALs performed as above. In selected experiments, cells from PLs or BALs were transferred to coverslips in a cytospin centrifuge and differentially stained with Differential Quik coloration.

Flow cytometry. Cells were obtained from BALs or PLs after centrifugation (700g, 15min, 4°C). When needed, red cells were lysed in ACK buffer (Invitrogen). Total viable cells were counted in a Vi-cell XR analyser (Beckman Coulter). Cells were washed in 1% BSA-PBS buffer and stained with Fixable Viability Dye eFluor506 (eBioscience). After blocking Fc receptors (anti-mouse CD16/32 antibody, 15 min, 4°C), cells were stained with the following anti-mouse antibodies in two independent mixes: anti-CD45 (clone: 30-F11) coupled to PE-Cy7, anti-CD11b (clone: M1/70) coupled to PerCP-Cy5.5, anti-CD11c (clone: HL3) coupled to Pacific Blue, anti-Siglec-F (clone: E50-2440) coupled to Alexa Fluor 647, anti-Ly6C (clone: AL-21) coupled to PE, anti-Ly6G (clone: 1A8) coupled to Alexa Fluor 700, anti-F4/80 (clon:BM8) coupled to eFluor450, anti-CD3 (clone:145-2C11) coupled to APC, anti-CD4 (clone:GK1.5) coupled to FITC, anti-CD8 (clone:53-6.7) coupled to PerCP-Cy5.5, anti-B220 (clone:RA3-6B2) coupled to PE, anti-CD19 (clone:1D3) coupled to Alexa Fluor 700, anti-NK1.1 (clone:PK136) coupled to APC-Cy7 (all antibodies were purchased from BioLegend except anti-SiglecF, anti-B220 and anti-CD19 which were from BD Biosciences, and anti-F4/80 and anti-NK1.1 which were from eBioscience). Staining was performed for 30 min, at 4°C in 1% BSA-PBS pH 7 buffer. After washing, cells were fixed in 2% PFA in PBS overnight at 4°C. Cell associated-fluorescence was acquired in a LSR Fortessa analyser (BD Biosciences) using Diva software. Analysis of % of alveolar

macrophages ($CD11c^{+}CD11b^{-/low}SiglecF^{+}$), peritoneal macrophages ($CD11b^{+}F4/80^{+}$), monocytes ($CD11c^{-}CD11b^{+}Ly6G^{-}Ly6C^{high}$), neutrophils ($CD11c^{-}CD11b^{+}Ly6G^{+}Ly6C^{dim}$), B-cells ($B220^{+}CD19^{+}$), T-CD4 ($CD3^{+}CD4^{+}$) and T-CD8 ($CD3^{+}CD8^{+}$) cells was performed excluding cell debris and doublets, in CD45 positive cells, using FlowJo program 10v (see gate strategy in Fig-S4). Cell numbers for each population in the BALs and PLs were obtained after multiplying its % (obtained by flow cytometry) by the total cell number (cell counting).

Viral loads in lungs. Lungs from infected mice were homogenized in PBS at 4°C using lysing matrix D tubes in a FastPrep-24 5G instrument (MP Biomedicals). 1/10 dilutions of lung homogenates were added to confluent MDCK cells and pfu obtained by the plaque assay (see above). Pfu were referred to total protein concentration (Micro BCA protein assay, Pierce) in lung homogenates.

Measurement of cytokines. Concentration of cytokines in cell cultures supernatants, mice BALs and PLs, were quantified by sandwich ELISA kits following the manufacturer's indications (R&D Bio-Techne).

RNA Extraction and RT-qPCR in lung homogenates. Frozen lungs were homogenized in RNA lysis buffer provided by the Pure Link RNA extraction kit (Life Technologies), using lysing matrix D tubes and FastPrep-24 5G mixer (MP Biomedical) at 4°C (two cycles of 40s, level 5). RNA isolation steps were performed according to the manufacturer's instructions (Life Technologies). The corresponding cDNA was synthesised using random hexamers (Roche) and M-MLV reverse transcriptase (Promega). Real-time PCR was performed in 7500 Fast Real-Time PCR System (Applied Biosystems) using the Fast SYBR Green Master Mix (Applied

Biosystems). The primers used were described in*[29]*. Triplicate Ct values were analysed using the comparative Ct (ΔΔCt) method. The amount of target ($2^{-\Delta\Delta CT}$) was calculated using control mice as calibrator (arbitrary units=1) and 18s rRNA (Fw:cttagagggacaagtggcg; Rw: acgctgagccagtcagtgta) as the house keeping gene.

Transmission electron microscopy. TEM was performed as described before*[30]* . A drop of a suspension containing AgNPs alone or previously mixed with KLH (at the same ratio used in vaccinal preparations) was laid on formvar/carbon-coated copper grids. After 5min, grids were stained with 1% uranyl acetate (1min) and then examined in a Tecnai12 (FEI, The Netherlands) transmission electron microscope at 80 kV equipped with a 1K×1K Keen View camera.

Antibody Titers. Specific antibody titers were obtained by ELISA. Maxisorb (Nunc) 96-well plates were coated with KLH (for detection of KLH specific antibodies) or cellular extracts of A549 cells infected with influenza virus (for detection of influenza specific antibodies) at 10µg/ml in carbonate/bicarbonate buffer pH 9.6 overnight at 4°C. After blocking non-specific binding in 5% skimmed milk in PBS, serial dilutions of BALs or serums were added in 1% skimmed milk, 0.05% Tween-20 in PBS (ELISA buffer) for 2h at 37°C. Afterwards, either anti-mouse IgA (1/2000) or anti-mouse IgG (1/4000) antibodies coupled to biotin (SouthernBiotech) were added in ELISA buffer for 2h at 37°C. Finally, wells were incubated with streptavidin coupled to alkaline phosphatase for 1h at 37°C. Enzymatic activity was detected after incubation with PNP substrate (Sigma) and measure of the OD was performed at 405nm. OD_{405nm} *versus* sample dilution for each mouse were plotted to obtain specific titers. Titers were defined as the reciprocal of the last dilution giving a value of OD over the double of the background (usually

values between 0.2 and 0.4). Mean+/-SEM of the reciprocal of the dilutions are represented in the corresponding figures. Titers represented in the same figure were obtained from an ELISA which included all samples represented.

*ELISPOT***.** MutiScreen-HA plates (Millipore-Merck) were coated with KLH (to detect KLH specific plasma cells) or a cellular extract from A549 cells infected with influenza A virus (to detect influenza specific plasma cells), as described for the detection of specific antibodies by ELISA (see above). Plates were washed with PBS and unspecific sites blocked with culture media (RPMI supplemented with 10% FCS and 5% penicillin/streptomycin) for 2h at 37°C. Cells isolated from spleens or para-tracheal lymph nodes were seeded in the wells by 2-fold serial dilution in culture media and incubated overnight at 37°C in a CO_2 incubator. Next, cells were removed with several PBS washes and remaining attached cells were lysed after incubations with H_20-Tween 0.05%. Next, plates were incubated with goat anti-mouse IgG-biotin or goat anti-mouse IgA-biotin (SouthernBiotech) for 2h at 37°C in 1% skimmed milk PBS-Tween 0.05% buffer. Plates were then washed and incubated with Streptavidin-coupled to phosphatase alkaline (PA) (SouthernBiotech) in the same buffer for 30 min at 37°C. Excess of streptavidin was removed and plates were incubated with Liquid Permanent Red (Dako) or BCP/NBT (Sigma) substrate. Plates were then washed with water and air-dried. Spots were quantified with binoculars and specific plasma cells were expressed in numbers per 100.000 lymphoid node/PBMC cells.

Immunohistochemistry. Perfused and fixed lungs (4% PFA in PBS, overnight at 4°C) were embedded in paraffin and sectioned in slides (4µm). After deparaffinization and rehydration, antigen retrieval was performed in citrate buffer (pH 6) for 40 min at 95°C. Slides were

sequentially incubated in 2% normal serum (from the species in which the secondary antibody was raised) and then in 1% BSA, 0.02% Triton X-100 (diluted in PBS). Samples were then treated with biotin blocking reagent (Vector Labs) and peroxidase blocking reagent (Dako). Antibodies used (1/200) were the following: rat anti-B220 (clone:RA3-6B2) (BioLegend), rabbit anti-mouse CD3 (clone: SP7) (Abcam), rat anti-mouse CD138 (clone:281-2) (BioLegend), rat anti-mouse MU/HU GL7 (clone:GL7) (BioLegend), goat anti-mouse IgA (SouthernBiotech). When double staining was performed on the same slice (CD3/B220), first antibody was incubated overnight at 4°C and developed with the corresponding secondary antibody biotinylated (Vector) using AP Vectastain ABC kit polymer (Vector Labs) to amplify the signal developed in Liquid Permanent Red (Dako). Co-staining was then performed using another primary antibody that was developed with the corresponding HRP-based polymer N-Histofine (Nichirei Biosciences) using DAB substrate (Dako). Biotinylated goat-anti rat IgM (Bethyl) was used as secondary antibody for develop GL7 positive cells. Finally, all slides were co-stained with haematoxylin (Sigma) and mounted with Aquatex medium (Merck Millipore). Image analysis was performed with a Leica DM4000 B microscopy equipped with a Leica DFC420 camera. Images were processed with ImageJ software.

Statistical analysis. Unless otherwise stated, data were expressed as means ± standard errors of the mean (SEM). Differences among groups were assessed using a Kruskal-Wallis test to compare more than two groups (followed by a Dunn's test for comparisons between groups) or a Mann–Whitney test to compare two groups. Analyses were performed with Prism version 7, GraphPad. Survival curves were compared with Log-Rank (Mantel-Cox) test.

Results

Characterization of silver nanoparticles.

Silver nanoparticles (AgNPs) of Biopure quality were obtained from Nanocomposix company which provided detailed data of their physico-chemical properties (summarized in Fig-1A). Further, we periodically confirmed the absence of NP aggregates by TEM (Fig-1B) and absorption spectroscopy (not shown). We also confirmed the absence of endotoxin in our preparation by the LAL (*Limulus* amebocyte lysate) at doses of AgNPs that did not interfere with the LAL assay (see M&M section), as described previously*[28]*. Moreover, to definitely rule out the presence of endotoxin as a contaminant in our AgNPs preparations, we stimulated bone marrow derived dendritic cells (BMDC) and alveolar macrophages (MPI cell line) with AgNPs. AgNPs did not induce the release of pro-inflammatory cytokines in either of these cells although both cell types were extremely sensitive to LPS (Fig-1C). To assess whether NPs could physically bind to our test antigens, we assayed the capacity of AgNPs to interact with the keyhole limpet hemocyanin (KLH) protein, a strongly immunogenic protein widely used as a model of vaccine antigen*[31]* , which we also used here in our protocols (see below). After mixing KLH and AgNPs, TEM images showed that AgNPs 'decorated' KLH aggregates (Fig-1D), demonstrating the capacity of AgNPs to complex with KLH protein.

Silver nanoparticles exert pro-inflammatory activity and enhance specific immunity against KLH protein during intraperitoneal immunization.

Most of the licensed adjuvants are pro-inflammatory molecules able to induce a local inflammatory response at the site of injection*[9,10]*. We sought to investigate whether intraperitoneal (i.p) injection of AgNPs in C57Bl/6 mice induced cellular recruitment and changes in the cytokine profile in the peritoneal lavage (PL) of treated mice. As indicated in Fig-2A, AgNPs induced neutrophil and monocyte recruitment and increased the levels of KC

(CXCL-1), IL-12 and IL-6, as soon as 4h after AgNPs injection. Importantly, as indicated above (Fig-1), this pro-inflammatory activity was not due to endotoxin contamination.

PL cytospins showed that AgNPs were internalized by macrophages and neutrophils, demonstrating that AgNPs target resident and recruited myeloid cells (Fig-2A). Considering the capacity of AgNPs to make complexes with KLH (Fig-1D) and their intrinsic pro-inflammatory activity (Fig-2A), we set-up a protocol (prime and boost at D0 and D8) to immunize C57Bl/6 mice i.p against KLH in the presence of AgNPs (Fig-2B). Analysis at D16 showed an enhanced production of KLH-specific IgG antibodies in the serum as well as increased numbers of KLH-specific IgG secreting plasma cells in the spleen, at a comparable extent to that obtained with Poly IC, a TLR-3 ligand used as positive control adjuvant (Fig-2C).

Intra-pulmonary delivery of silver nanoparticles induces transient inflammation.

Having demonstrated that AgNPs have intra-peritoneal adjuvant activity, we next sought to investigate the effect of these nanoparticles in the lung. First, AgNPs (1mg/Kg) were instilled intra-tracheally (i.t) in C57Bl/6 mice. A kinetic study indicated that AgNPs treatment increased the levels of CCL-5, CCL-2, IL-12 and IL-6 in the broncho-alveolar lavages (BALs) at day-1 (D1) post-instillation (Fig-3A). This increase in pro-inflammatory cytokines and chemokines was accompanied by a neutrophil recruitment in the BALs (Fig-3B). In addition, we observed in cytospin samples that alveolar macrophages (AM) internalized AgNPs (Fig-3B, white asterisk). Interestingly, levels of all these pro-inflammatory parameters decreased D3 post-instillation with the exception of IL-12 which remained up-regulated (Fig-3A), the latter correlating with T cell recruitment in the BALs at D3 (Fig-3B).

Silver nanoparticles enhance mucosal specific immunity against KLH and reorganize lung immunity during pulmonary immunization.

Having demonstrated that AgNPs can induce IL-12, concomitantly with a transient pulmonary innate (at D1), and adaptive (at day D3) cell influx, we tested whether this activity could be harnessed to increase local mucosal immunity against KLH (see protocol for i.t immunisation in Fig-4A). Ten days after the last boost (D20), BAL KLH-specific IgA and IgG antibodies were shown to be increased only in the group of mice immunized with KLH/AgNPs mixture (Fig-4B). Moreover, only in this group KLH-specific IgG were also increased in the serum (Fig-4B).

In parallel, T and B cells levels were drastically increased in the BALs of KLH/AgNPs immunised animals, compared to the KLH- or AgNPs- immunised groups (Fig-4C). KLH/AgNPs immunisation also increased protein levels of IL-12 and BAFF (a survival factor for B-cells promoting B-cell maturation) (Fig-4C). Echoing the presence of specific antibodies and BAFF in BALs, specific plasma cells were only detected in the paratracheal LN from the KLH/AgNPs immunized group (Fig-4D). Furthermore, only in the lung parenchyma of KLH/AgNPs immunised animals cellular aggregates (lineating bronchi) were clearly seen (Fig-4E), without any signs for acute inflammation (as evidenced by lack of neutrophil recruitment). Staining with specific antibodies clearly demonstrated that these aggregates were composed of T and B cells ($CD3^+$ and $B220^+$ cells, respectively) (Fig-4E), suggesting that these structures might represent early inducible BALT (iBALT) induced following lung infection*[32]* .

Overall, these data indicate that lung vaccination with AgNPs used as an adjuvant induces both local and systemic immunity against KLH, potentially through the organisation of tertiary lymphoid organs.

Pulmonary immunization with heat-killed influenza virus in the presence of silver nanoparticles protects mice against sub-lethal flu.

Building on the above observations that AgNPs increased mucosal immunity against the model antigen KLH, we then studied the changes in local immunity induced by i.t immunization with an AgNPs-flu vaccine, using heat-inactivated influenza A virus (IAV*) as vaccine antigen. We observed that after the end of the immunization period (D20, Fig-S1A), only mice immunized with IAV* plus AgNPs (IAV*/AgNPs) recruited T-CD4 and B-cells and presented increased levels of IL-12 and BAFF in the BALs compared to mice immunized in the absence of adjuvant (IAV* only group) (Fig-S1B), as we observed previously during pulmonary KLH/AgNPs immunisation (Fig-4C). Remarkably, vaccination with IAV*/AgNPs was associated with the presence of T/B-cell aggregates in the lung parenchyma (Fig-S1C), specific antibodies in the BALs (Fig-S1D) and with local increased expression of CCL-20, CCL-21, CXCL-13 and CXCL-16 (Fig-S1E), all cytokines/chemokines that participate in the initiation and maintaining of iBALT *[33,34]* . Altogether, these data confirm that vaccination with IAV* (or KLH) in the presence of AgNPs stimulates lung mucosal immunity through induction of iBALT.

We then performed vaccination/challenge experiments (Fig-5A) whereby animals vaccinated as above with IAV*/AgNPs mixtures were then challenged with sub-lethal doses of the same strain of live IAV virus (300 pfu). After infection, mice not vaccinated or immunized with IAV* alone lost weight (an accepted sign of the severity of the infection) whereas vaccination with IAV*/AgNPs protected mice from body weight loss (Fig-5B). Concomitantly, viral loads in the lungs of IAV*/AgNPs mice were significantly reduced at D28 (d8pi), compared to mice vaccinated with unadjuvanted IAV* (Fig-5C). At the cellular level, as expected, live IAV induced the recruitment of neutrophils, monocytes and T-cells and increased the levels of IFN-γ

in the BALs, compared to non-infected animals (Fig-5D). Interestingly, mice vaccinated with IAV*/AgNPs presented at d8pi a sharp reduction in neutrophils, monocytes and T-cells influx, as well as a decrease in BAL IFN-γ levels, when compared to mice vaccinated with unadjuvanted IAV* (Fig-5D). Remarkably, the protective phenotype observed in the IAV*/AgNP vaccinated group was associated with the highest levels of anti-IAV IgA and IgG antibodies in the BALs and serum (Fig-5E).

Altogether, these data indicated that flu vaccination with AgNPs reduces viral replication, increases mucosal IgA and IgG titers, and protects against body weight loss, while down-regulating influenza-induced lung inflammation.

Silver nanoparticles are superior in inducing specific lung IgA production and germinal centers development compared to other adjuvants during flu vaccination.

We then compared the adjuvanticity of AgNPs with other commonly used adjuvants, *e.g.* Poly IC (TLR-3 ligand) used in experimental flu vaccines*[35,36]* and AddaVax, a squalene-based oil-in-water emulsion of similar composition as MF59, used in parenteral injections of human flu vaccines*[11]*. Using the same protocol as described in Fig-5A, we showed that all 3 adjuvants protected mice from IAV-induced body weight loss, compared to mice immunized with IAV* only (Fig-6A). Concomitantly, at d8pi, IAV-mediated lung inflammation (as evidenced by neutrophil, monocyte influx and IFNγ production) was drastically reduced at d8pi in immunized mice, regardless of the adjuvant, when compared to the non-adjuvated group (IAV*) (Fig-6B). In particular, monocytes were almost absent in the IAV*/AgNPs vaccinated group. Importantly, we only found increased numbers of B-cells in the BALs of the latter group (Fig-6B), suggesting that AgNPs could specifically favour B-cell recruitment to the lungs. Echoing this, regardless of the

adjuvant, global anti-IAV titers were higher in the 'adjuvant'/IAV* groups, compared to the non-adjuvated group (IAV*). However, whereas Poly IC increased anti-IAV IgG titers in d8pi BALs, it modestly increased anti-IAV IgA titers. AgNPs were a far better IAV-specific IgA inducer compared to Poly IC or AddaVax (Fig-6C). In accordance, IAV-specific IgA secreting plasma cells numbers were clearly increased in IAV*/AgNPs immunized mice compared to IAV* or IAV*/Poly IC groups (Fig-6C), demonstrating that the AgNPs adjuvant activity was clearly associated to mucosal induction of specific anti-IgA antibodies.

Because AgNPs lung treatment in the context of antigen exposure (either KLH, Fig-4, or IAV*, Fig-S1C) induces the relevant cytokine milieu (Fig-S1E) for the initiation and maintaining of iBALT, we further studied, in the context of live IAV infection, the presence of these structures in lung sections. As early as d8pi, live IAV infection of mice (vaccinated with unadjuvanted IAV*) induced T and B cells influx in lung parenchyma, in an 'unorganized' fashion, as previously shown*[37]* (Fig-6D, top left panel). In accordance, these T/B-cell 'mini-aggregates' were only faintly positive for GL-7 (Fig-6D, top right panel), a known marker of germinal centers (GC) in secondary lymphoid organs and tertiary lymphoid organs (TLOs)*[37,38]*. Similarly, vaccination with AddaVax also induced T/B infiltrates, but with a similar low expression of GL-7. By contrast, infection of IAV*/PolyIC immunized mice clearly induced some organization of the T/B-cell aggregates in the lung but again, their GL-7 expression was minimal (Fig-6D, middle panels). Remarkably, only in the IAV*/AgNPs group was a clear organization of these T/B-cell aggregates observed, concomitantly with strong GL-7 positivity (Fig-6D, bottom panels). Quantification of T/B-cell aggregates (only counting those containing 15 or more positive cells) confirmed that, as early as d8pi, vaccination with IAV*/AgNPs clearly increased the number of B-cell aggregates and, even more importantly, that of GC (GL-7^+ aggregates) (Fig-6D, right histograms) compared to mice vaccinated only with IAV*.

Vaccination with silver nanoparticles or silver salts protects mice from lethal flu.

In order to measure the amplitude of the protection conferred by the AgNPs-adjuvanted flu vaccine, mice were immunized (same protocol as described in Fig-5A) and then challenged with a lethal dose of influenza virus (1000 pfu). Moreover, to demonstrate that silver was critical in the processes described here, and to discriminate between the potential effect of the 'silver core' (in the context of the nanoparticle itself) *versus* that of 'free' silver ions, a further comparative study was performed, adding gold nanoparticles (AuNPs), and silver nitrates salts ($AgNO_3$), as additional arms to the experimental protocol. Survival curves of infected mice showed that all mice immunized with IAV* alone died by d10pi (Fig-7A). Importantly, whereas mice immunized with IAV*/AuNPs did not survive significantly longer, immunization with silver nitrates ($AgNO_3$) ameliorated survival compared to the IAV*-alone immunized group (Fig-7A). Remarkably, all mice immunised with AgNPs survived, and at d18pi, anti-IAV IgA were detected in the BALs of surviving animals from both IAV*/AgNPs and IAV*/$AgNO_3$ immunized groups (Fig-7B). Furthermore, although the actual numbers of B-cell, GC ($GL7^+$) and $CD138^+$ cells (a marker for antibody secreting plasma cells*[39]*) aggregates were equivalent in the lung parenchyma of surviving mice from both IAV*/$AgNO_3$ and IAV*/AgNPs groups, the size of B-cell aggregates and GC were bigger in the latter group (Fig-7C). These data indicate that active GC ($GL\text{-}7^+$) are probably overall more efficient in IAV*/AgNPs immunized mice since we only found cells actively secreting IgA ($B220^-CD138^+IgA^+$) in the lung parenchyma of that group of mice (Fig-7D).

Discussion

The use of nanomaterials has recently been suggested to improve vaccine efficacy*[12]*, likely because of a depot effect associated to a prolonged maintaining of antigens at entry sites[13–15]. In addition, the intrinsic antimicrobial properties of metallic nanoparticles such as AgNPs (either through direct interaction with microbial surfaces and/or because of their interference with their metabolism)*[40]* is a further argument for their use in anti-infective vaccines. Consistent with this notion, AgNPs have been shown to enhance the production of ovalbumin (OVA) specific IgG antibodies in the serum of mice parenterally immunized with OVA*[41]* and to adjuvate a rabies vaccine administered intraperitoneally in mice*[42]*, albeit through undeciphered mechanisms.

However, despite these advances, it is increasingly being recognized that these systemic route of administration of adjuvants/antigen do not favour robust immune mucosal responses, contrary to local administration[1–3].

We show here that AgNPs can physically bind and sequester the model antigen KLH (Fig-1) as well as heat-killed IAV capsids (not shown). When administered intra-pulmonary, we showed that this increased antigen availability could result in better retention of the antigen in the lung compartment (as shown before*[43]*), and resulted in enhanced local immune stimulation. Mechanistically, pulmonary administration of AgNPs induced transient local inflammation *in vivo* (Fig-3) resulting in upregulation of IL-12. Although macrophages and DCs are classically considered as potential sources of IL-12*[44]*, a cytokine that could be induced by direct APC activation by the adjuvant, the IL-12 secretion observed in our model probably resulted from an indirect activation of these cells by the pro-inflammatory milieu favoured after AgNPs instillation, since AgNPs alone did not stimulate their IL-12 secretion *in vitro* (Fig-1C). Indeed, similarly to AgNPs, other adjuvants, such as MF59 or aluminium derivates, were also shown to activate DC indirectly*[9]*.

Although a variety of adjuvants could potentially be used for lung immunization purposes, we showed here, using either KLH or inactivated IAV as 'model antigens', that compared to polyIC and AddaVax, AgNPs were indeed superior at inducing specific IgA antibodies, when given i.t (Fig-6). In particular, AddaVax was found to be a poor adjuvant, and furthermore, its administration by the respiratory route resulted in elevated toxicity during the immunisation process (as evidenced by loss of body weight) (Fig-S2), even though it was used at less than half of the dose recommended for parenteral administration.

Crucially, and importantly for fostering mucosal immunity, the production of anti-IAV IgA antibodies was particularly impressive following AgNPs/KLH (Fig-4) or AgNPs/IAV* (Fig-5) immunisations. Indeed, the B-cell survival factor BAFF*[45]* was elevated in BALs of mice immunized with these combinations, when compared to antigen alone (Fig-4C and S1B). This was accompanied by the recruitment of B-cells in the BALs, independently of the antigen tested (Fig-4 and S1), even after infection with live IAV (Fig-6B). This recruitment was likely the consequence of local B cell production, as assessed by increased numbers of plasma cells in both paratracheal lymph nodes, and in the lung parenchyma (Fig 4D-E; Fig 6C-D). Importantly, increased IgA secreting plasma cells correlated with elevated titers of specific IgA antibodies in the BALs. Comparison of AgNPs with other adjuvants (experimental or licensed), demonstrated that AgNPs induced stronger specific IgA production (antibodies or plasma cells).

Likely explaining the induced IgA and specific plasma cell generation, we demonstrated that compared to other adjuvant mixtures, vaccination with AgNPs/KLH or AgNPs/IAV* accelerated the formation of T/B cell aggregates within the lung parenchyma (Figs 4E, 6D) and that of germinal centers (GC) in these structures, therefore defining the latter as *bona fide* iBALT. The capacity of IAV*/AgNPs vaccine to induce/accelerate GC formation during influenza infection could be related to the upregulation of CCL-20, CXCL-13 and CXCL-16*[33,34]* chemokines

(which attract B-cells, T-cells and DC) (Fig-S1E). Indeed, and consistent with the upregulation of these cytokines involved in iBALT development, we only found T/B aggregates in the lung parenchyma of antigen/AgNPs vaccinated mice (Fig-4E, Fig-S1C). Crucially, the AgNPs/IAV* vaccination protocol was associated with complete protection against live IAV-challenged mice, and the surviving mice maintained at d8pi strong IgA expression (Fig-5E) and the GCs organization within their lungs (Fig-7C).

Mechanistically, the 'silver core' (in the context of the nanoparticle itself) was shown to be superior (and less toxic (Fig- S3)) to 'free' silver ions in eliciting GC organization at mucosal sites (Fig-7C), likely because of its capacity to physically bind the antigen (Fig-1 for KLH and data not shown for IAV*) thereby probably increasing its *in vivo* half-life and 'visibility' to the immune system. Because pulmonary administration of AgNPs has been associated with toxicity specially in those cells that first encounter AgNPs (*e.g.* AMs)([20] and Fig-3) and since release of Damage Associated Molecular Patter molecules (DAMPs) by dead cells could contribute to immunogenicity [46], we measured the impact of AgNPs administration in AM viability (Fig-S5). We observed that the latter was not affected by intracheal instillation of AgNPs, ruling out the possibility that local cell death induced by AgNPs substantially contributed to AgNPs immunogenicity. Other mechanisms of action not explored in our study could be related to the capacity of AgNPs to promote cellular uptake of the antigen by APC, to enhance lymphatic drainage of the antigen, and to facilitate antigen/adjuvant delivery at secondary lymphoid organs, as described for other particulate adjuvants[23,47,48].

In conclusion, our data demonstrate for the first time the unique property of the silver core of AgNPs in shaping lung iBALT, and in fostering IgA-mediated lung immunity. Importantly, induction of iBALT during influenza infection in murine models has already been associated to a better protection against flu*[38,49]*, further validating the search for adjuvants (like AgNPs) able

to generate these tertiary lymphoid structures. Despite the well-recognized importance of other arms of immunity to fight Influenza infections (for a recent review, see McMichael *et al.[50]*), we believe that our data therefore strengthens the emerging concept that particulate vaccine formulations favouring Th2/IgA responses*[51,52]* and including AgNPs may be of potential use as new prophylactic agents.

Acknowledgements

Funding: this work was supported by the French National Agency of Research (ANR-13-JS10-0007-01). We thank Olivier Thibaudeau from the histology platform (Inserm U1152, Bichat) for his help in tissue processing. We also thank people from the animal facility (CRI -U1149) and the flow cytometry platforms (CRI -U1149) who contribute to the maintenance of those facilities. Authors also acknowledge Dr Gyorgy Fejer (University of Plymouth, United Kingdom) for providing the MPI cells. We thank Prof Zhou Xing (MacMaster University, Hamilton, Canada) for helpful discussions and a critical reading of the manuscript.

Author contributions

Investigation S.G.D., L.G.P., V.B., S.N., K.A. and G.V.I.; Methodology V.B. and L.B.R.; Resources, L.B.R., G.A.; Writing-Original draft S.J.M. and G.V.I.; Writing-Reviewing&Editing, G.A., C.B., S.J.M. and I.G.V.; Supervision: G.V.I.; Funding: C.B. and S.J.M.

Supporting information

File: "Supplementary Figures and Legends.pdf". Legends and Figures S1to S5.

REFERENCES

[1] K. Sano, A. Ainai, T. Suzuki, H. Hasegawa, The road to a more effective influenza vaccine: Up to date studies and future prospects, Vaccine. 35 (2017) 5388–5395. doi:10.1016/j.vaccine.2017.08.034.

[2] J.L.K. Wee, J.-P.Y. Scheerlinck, K.J. Snibson, S. Edwards, M. Pearse, C. Quinn, P. Sutton, Pulmonary delivery of ISCOMATRIX influenza vaccine induces both systemic and mucosal immunity with antigen dose sparing, Mucosal Immunol. 1 (2008) 489–496. doi:10.1038/mi.2008.59.

[3] T. Suzuki, A. Ainai, H. Hasegawa, Functional and structural characteristics of secretory IgA antibodies elicited by mucosal vaccines against influenza virus, Vaccine. 35 (2017) 5297–

5302. doi:10.1016/j.vaccine.2017.07.093.

[4] S.-I. Tamura, A. Ainai, T. Suzuki, T. Kurata, H. Hasegawa, Intranasal Inactivated Influenza Vaccines: a Reasonable Approach to Improve the Efficacy of Influenza Vaccine?, Jpn. J. Infect. Dis. 69 (2016) 165–179. doi:10.7883/yoken.JJID.2015.560.

[5] K. Chen, A. Cerutti, Vaccination strategies to promote mucosal antibody responses, Immunity. 33 (2010) 479–491. doi:10.1016/j.immuni.2010.09.013.

[6] J. Mestecky, M.W. Russell, C.O. Elson, Perspectives on mucosal vaccines: is mucosal tolerance a barrier?, J. Immunol. 179 (2007) 5633–5638.

[7] A.A. Timothy, A. Tokanovic, K.J. Snibson, S.J. Edwards, M.J. Pearse, J.-P.Y. Scheerlinck, P. Sutton, ISCOMATRIX™ adjuvant reduces mucosal tolerance for effective pulmonary vaccination against influenza, Hum Vaccin Immunother. 11 (2015) 377–385. doi:10.4161/21645515.2014.990859.

[8] X.-Z.J. Guo, P.G. Thomas, New fronts emerge in the influenza cytokine storm, Semin Immunopathol. 39 (2017) 541–550. doi:10.1007/s00281-017-0636-y.

[9] G. Del Giudice, R. Rappuoli, A.M. Didierlaurent, Correlates of adjuvanticity: A review on adjuvants in licensed vaccines, Semin. Immunol. (2018). doi:10.1016/j.smim.2018.05.001.

[10] S. Awate, L.A. Babiuk, G. Mutwiri, Mechanisms of action of adjuvants, Front Immunol. 4 (2013) 114. doi:10.3389/fimmu.2013.00114.

[11] E.-J. Ko, S.-M. Kang, Immunology and efficacy of MF59-adjuvanted vaccines, Hum Vaccin Immunother. (2018) 1–5. doi:10.1080/21645515.2018.1495301.

[12] T.G. Dacoba, A. Olivera, D. Torres, J. Crecente-Campo, M.J. Alonso, Modulating the immune system through nanotechnology, Semin. Immunol. 34 (2017) 78–102. doi:10.1016/j.smim.2017.09.007.

[13] S. Okamoto, M. Matsuura, T. Akagi, M. Akashi, T. Tanimoto, T. Ishikawa, M. Takahashi,

K. Yamanishi, Y. Mori, Poly(gamma-glutamic acid) nano-particles combined with mucosal influenza virus hemagglutinin vaccine protects against influenza virus infection in mice, Vaccine. 27 (2009) 5896–5905. doi:10.1016/j.vaccine.2009.07.037.

[14] J. Hiremath, K. Kang, M. Xia, M. Elaish, B. Binjawadagi, K. Ouyang, S. Dhakal, J. Arcos, J.B. Torrelles, X. Jiang, C.W. Lee, G.J. Renukaradhya, Entrapment of H1N1 Influenza Virus Derived Conserved Peptides in PLGA Nanoparticles Enhances T Cell Response and Vaccine Efficacy in Pigs, PLoS ONE. 11 (2016) e0151922. doi:10.1371/journal.pone.0151922.

[15] S.M. Singh, T.N. Alkie, É. Nagy, R.R. Kulkarni, D.C. Hodgins, S. Sharif, Delivery of an inactivated avian influenza virus vaccine adjuvanted with poly(D,L-lactic-co-glycolic acid) encapsulated CpG ODN induces protective immune responses in chickens, Vaccine. 34 (2016) 4807–4813. doi:10.1016/j.vaccine.2016.08.009.

[16] A.L. Silva, C. Peres, J. Conniot, A.I. Matos, L. Moura, B. Carreira, V. Sainz, A. Scomparin, R. Satchi-Fainaro, V. Préat, H.F. Florindo, Nanoparticle impact on innate immune cell pattern-recognition receptors and inflammasomes activation, Semin. Immunol. 34 (2017) 3–24. doi:10.1016/j.smim.2017.09.003.

[17] C. Carlson, S.M. Hussain, A.M. Schrand, L.K. Braydich-Stolle, K.L. Hess, R.L. Jones, J.J. Schlager, Unique cellular interaction of silver nanoparticles: size-dependent generation of reactive oxygen species, J Phys Chem B. 112 (2008) 13608–13619. doi:10.1021/jp712087m.

[18] E.-J. Yang, S. Kim, J.S. Kim, I.-H. Choi, Inflammasome formation and IL-1β release by human blood monocytes in response to silver nanoparticles, Biomaterials. 33 (2012) 6858–6867. doi:10.1016/j.biomaterials.2012.06.016.

[19] J.-C. Simard, F. Vallieres, R. de Liz, V. Lavastre, D. Girard, Silver nanoparticles induce degradation of the endoplasmic reticulum stress sensor activating transcription factor-6 leading to activation of the NLRP-3 inflammasome, J. Biol. Chem. 290 (2015) 5926–5939.

doi:10.1074/jbc.M114.610899.

[20] N. Haberl, S. Hirn, A. Wenk, J. Diendorf, M. Epple, B.D. Johnston, F. Krombach, W.G. Kreyling, C. Schleh, Cytotoxic and proinflammatory effects of PVP-coated silver nanoparticles after intratracheal instillation in rats, Beilstein J Nanotechnol. 4 (2013) 933–940. doi:10.3762/bjnano.4.105.

[21] F. Alessandrini, A. Vennemann, S. Gschwendtner, A.U. Neumann, M. Rothballer, T. Seher, M. Wimmer, S. Kublik, C. Traidl-Hoffmann, M. Schloter, M. Wiemann, C.B. Schmidt-Weber, Pro-Inflammatory versus Immunomodulatory Effects of Silver Nanoparticles in the Lung: The Critical Role of Dose, Size and Surface Modification, Nanomaterials (Basel). 7 (2017). doi:10.3390/nano7100300.

[22] H.-W. Chen, C.-Y. Huang, S.-Y. Lin, Z.-S. Fang, C.-H. Hsu, J.-C. Lin, Y.-I. Chen, B.-Y. Yao, C.-M.J. Hu, Synthetic virus-like particles prepared via protein corona formation enable effective vaccination in an avian model of coronavirus infection, Biomaterials. 106 (2016) 111–118. doi:10.1016/j.biomaterials.2016.08.018.

[23] H. Li, K. Fierens, Z. Zhang, N. Vanparijs, M.J. Schuijs, K. Van Steendam, N. Feiner Gracia, R. De Rycke, T. De Beer, A. De Beuckelaer, S. De Koker, D. Deforce, L. Albertazzi, J. Grooten, B.N. Lambrecht, B.G. De Geest, Spontaneous Protein Adsorption on Graphene Oxide Nanosheets Allowing Efficient Intracellular Vaccine Protein Delivery, ACS Appl. Mater. Interfaces. 8 (2016) 1147–1155. doi:10.1021/acsami.5b08963.

[24] G. Fejer, M.D. Wegner, I. Györy, I. Cohen, P. Engelhard, E. Voronov, T. Manke, Z. Ruzsics, L. Dölken, O. Prazeres da Costa, N. Branzk, M. Huber, A. Prasse, R. Schneider, R.N. Apte, C. Galanos, M.A. Freudenberg, Nontransformed, GM-CSF-dependent macrophage lines are a unique model to study tissue macrophage functions, Proc. Natl. Acad. Sci. U.S.A. 110 (2013) E2191-2198. doi:10.1073/pnas.1302877110.

[25] N. Riteau, L. Baron, B. Villeret, N. Guillou, F. Savigny, B. Ryffel, F. Rassendren, M. Le Bert, A. Gombault, I. Couillin, ATP release and purinergic signaling: a common pathway for particle-mediated inflammasome activation, Cell Death Dis. 3 (2012) e403. doi:10.1038/cddis.2012.144.

[26] D. Barbier, I. Garcia-Verdugo, J. Pothlichet, R. Khazen, D. Descamps, K. Rousseau, D. Thornton, M. Si-Tahar, L. Touqui, M. Chignard, J.-M. Sallenave, Influenza A induces the major secreted airway mucin MUC5AC in a protease-EGFR-extracellular regulated kinase-Sp1-dependent pathway, Am. J. Respir. Cell Mol. Biol. 47 (2012) 149–157. doi:10.1165/rcmb.2011-0405OC.

[27] B. Villeret, A. Dieu, M. Straube, B. Solhonne, P. Miklavc, S. Hamadi, R. Le Borgne, A. Mailleux, X. Norel, J. Aerts, D. Diallo, F. Rouzet, P. Dietl, J.-M. Sallenave, I. Garcia-Verdugo, Silver Nanoparticles Impair Retinoic Acid-Inducible Gene I-Mediated Mitochondrial Antiviral Immunity by Blocking the Autophagic Flux in Lung Epithelial Cells, ACS Nano. 12 (2018) 1188–1202. doi:10.1021/acsnano.7b06934.

[28] M. Delaval, S. Boland, B. Solhonne, M.-A. Nicola, S. Mornet, A. Baeza-Squiban, J.-M. Sallenave, I. Garcia-Verdugo, Acute exposure to silica nanoparticles enhances mortality and increases lung permeability in a mouse model of Pseudomonas aeruginosa pneumonia, Part Fibre Toxicol. 12 (2015) 1. doi:10.1186/s12989-014-0078-9.

[29] K. Guedj, J. Khallou-Laschet, M. Clement, M. Morvan, A.-T. Gaston, G. Fornasa, J. Dai, M. Gervais-Taurel, G. Eberl, J.-B. Michel, G. Caligiuri, A. Nicoletti, M1 macrophages act as LTβR-independent lymphoid tissue inducer cells during atherosclerosis-related lymphoid neogenesis, Cardiovasc. Res. 101 (2014) 434–443. doi:10.1093/cvr/cvt263.

[30] I. Garcia-Verdugo, M. Synguelakis, J. Degrouard, C.-A. Franco, B. Valot, M. Zivy, R. Chaby, Z. Tanfin, Interaction of surfactant protein A with the intermediate filaments desmin and

vimentin, Biochemistry. 47 (2008) 5127–5138. doi:10.1021/bi800070u.

[31] A. Swaminathan, R.M. Lucas, K. Dear, A.J. McMichael, Keyhole limpet haemocyanin - a model antigen for human immunotoxicological studies, Br J Clin Pharmacol. 78 (2014) 1135–1142. doi:10.1111/bcp.12422.

[32] J.Y. Hwang, T.D. Randall, A. Silva-Sanchez, Inducible Bronchus-Associated Lymphoid Tissue: Taming Inflammation in the Lung, Front Immunol. 7 (2016) 258. doi:10.3389/fimmu.2016.00258.

[33] J. Rangel-Moreno, J.E. Moyron-Quiroz, L. Hartson, K. Kusser, T.D. Randall, Pulmonary expression of CXC chemokine ligand 13, CC chemokine ligand 19, and CC chemokine ligand 21 is essential for local immunity to influenza, Proc. Natl. Acad. Sci. U.S.A. 104 (2007) 10577–10582. doi:10.1073/pnas.0700591104.

[34] F. Perros, P. Dorfmüller, D. Montani, H. Hammad, W. Waelput, B. Girerd, N. Raymond, O. Mercier, S. Mussot, S. Cohen-Kaminsky, M. Humbert, B.N. Lambrecht, Pulmonary lymphoid neogenesis in idiopathic pulmonary arterial hypertension, Am. J. Respir. Crit. Care Med. 185 (2012) 311–321. doi:10.1164/rccm.201105-0927OC.

[35] T. Ichinohe, I. Watanabe, S. Ito, H. Fujii, M. Moriyama, S.-I. Tamura, H. Takahashi, H. Sawa, J. Chiba, T. Kurata, T. Sata, H. Hasegawa, Synthetic double-stranded RNA poly(I:C) combined with mucosal vaccine protects against influenza virus infection, J. Virol. 79 (2005) 2910–2919. doi:10.1128/JVI.79.5.2910-2919.2005.

[36] H. Takaki, S. Kure, H. Oshiumi, Y. Sakoda, T. Suzuki, A. Ainai, H. Hasegawa, M. Matsumoto, T. Seya, Toll-like receptor 3 in nasal CD103+ dendritic cells is involved in immunoglobulin A production, Mucosal Immunol. 11 (2018) 82–96. doi:10.1038/mi.2017.48.

[37] C.H. GeurtsvanKessel, M.A.M. Willart, I.M. Bergen, L.S. van Rijt, F. Muskens, D. Elewaut, A.D.M.E. Osterhaus, R. Hendriks, G.F. Rimmelzwaan, B.N. Lambrecht, Dendritic cells

are crucial for maintenance of tertiary lymphoid structures in the lung of influenza virus-infected mice, J. Exp. Med. 206 (2009) 2339–2349. doi:10.1084/jem.20090410.

[38] J.E. Moyron-Quiroz, J. Rangel-Moreno, K. Kusser, L. Hartson, F. Sprague, S. Goodrich, D.L. Woodland, F.E. Lund, T.D. Randall, Role of inducible bronchus associated lymphoid tissue (iBALT) in respiratory immunity, Nat. Med. 10 (2004) 927–934. doi:10.1038/nm1091.

[39] K.G. Smith, T.D. Hewitson, G.J. Nossal, D.M. Tarlinton, The phenotype and fate of the antibody-forming cells of the splenic foci, Eur. J. Immunol. 26 (1996) 444–448. doi:10.1002/eji.1830260226.

[40] H.H. Lara, E.N. Garza-Treviño, L. Ixtepan-Turrent, D.K. Singh, Silver nanoparticles are broad-spectrum bactericidal and virucidal compounds, J Nanobiotechnology. 9 (2011) 30. doi:10.1186/1477-3155-9-30.

[41] Y. Xu, H. Tang, J.-H. Liu, H. Wang, Y. Liu, Evaluation of the adjuvant effect of silver nanoparticles both in vitro and in vivo, Toxicol. Lett. 219 (2013) 42–48. doi:10.1016/j.toxlet.2013.02.010.

[42] V. Asgary, A. Shoari, F. Baghbani-Arani, S.A. Sadat Shandiz, M.S. Khosravy, A. Janani, R. Bigdeli, R. Bashar, R.A. Cohan, Green synthesis and evaluation of silver nanoparticles as adjuvant in rabies veterinary vaccine, Int J Nanomedicine. 11 (2016) 3597–3605. doi:10.2147/IJN.S109098.

[43] D.S. Anderson, R.M. Silva, D. Lee, P.C. Edwards, A. Sharmah, T. Guo, K.E. Pinkerton, L.S. Van Winkle, Persistence of silver nanoparticles in the rat lung: Influence of dose, size, and chemical composition, Nanotoxicology. 9 (2015) 591–602. doi:10.3109/17435390.2014.958116.

[44] A.K.A. Wright, D.E. Briles, D.W. Metzger, S.B. Gordon, Prospects for use of interleukin-12 as a mucosal adjuvant for vaccination of humans to protect against respiratory pneumococcal infection, Vaccine. 26 (2008) 4893–4903. doi:10.1016/j.vaccine.2008.06.058.

[45] C.R. Smulski, H. Eibel, BAFF and BAFF-Receptor in B Cell Selection and Survival, Front Immunol. 9 (2018) 2285. doi:10.3389/fimmu.2018.02285.

[46] T. Nakayama, An inflammatory response is essential for the development of adaptive immunity-immunogenicity and immunotoxicity, Vaccine. 34 (2016) 5815–5818. doi:10.1016/j.vaccine.2016.08.051.

[47] M.F. Bachmann, G.T. Jennings, Vaccine delivery: a matter of size, geometry, kinetics and molecular patterns, Nature Reviews Immunology. 10 (2010) 787–796. doi:10.1038/nri2868.

[48] S. Chattopadhyay, J.-Y. Chen, H.-W. Chen, C.-M.J. Hu, Nanoparticle Vaccines Adopting Virus-like Features for Enhanced Immune Potentiation, Nanotheranostics. 1 (2017) 244–260. doi:10.7150/ntno.19796.

[49] J.E. Moyron-Quiroz, J. Rangel-Moreno, L. Hartson, K. Kusser, M.P. Tighe, K.D. Klonowski, L. Lefrançois, L.S. Cauley, A.G. Harmsen, F.E. Lund, T.D. Randall, Persistence and responsiveness of immunologic memory in the absence of secondary lymphoid organs, Immunity. 25 (2006) 643–654. doi:10.1016/j.immuni.2006.08.022.

[50] A.J. McMichael, Legacy of the influenza pandemic 1918: The host T cell response, Biomed J. 41 (2018) 242–248. doi:10.1016/j.bj.2018.08.003.

[51] A. Lamichhane, T. Azegamia, H. Kiyonoa, The mucosal immune system for vaccine development, Vaccine. 32 (2014) 6711–6723. doi:10.1016/j.vaccine.2014.08.089.

[52] E. Kuroda, C. Coban, K.J. Ishii, Particulate adjuvant and innate immunity: past achievements, present findings, and future prospects, Int. Rev. Immunol. 32 (2013) 209–220. doi:10.3109/08830185.2013.773326.

A)

	Coating	Diameter (nm)	Hydrodynamic Diameter (nm)	Zeta potential (mV)	Endotoxin (EU/ml)
AgNPs	Lipoic acid	10.3 ± 2.0	18	-37	< 5
AuNPs	Lipoic acid	7.9 ± 0.8	n.r.	n.r.	< 2.5

B)

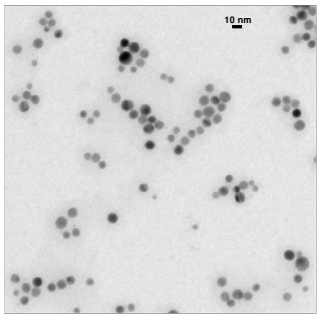

C)

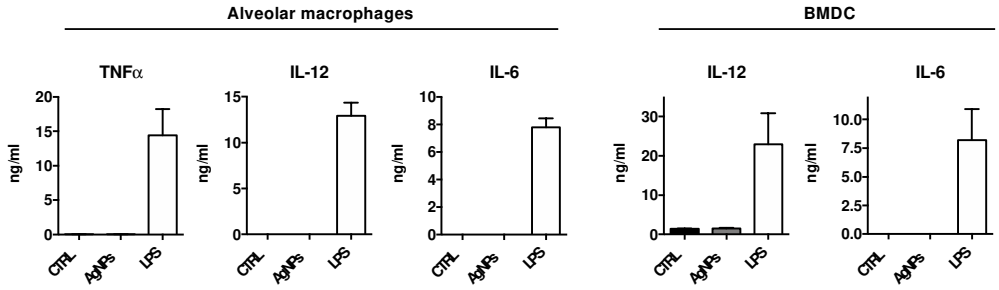

D)

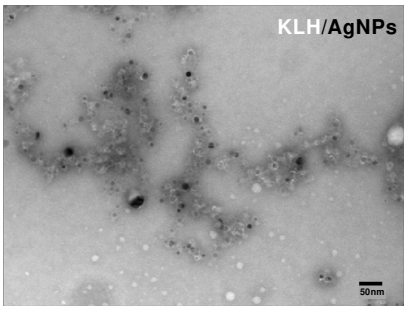

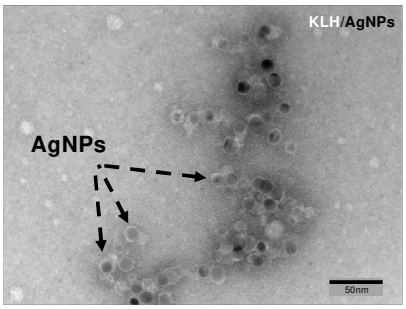

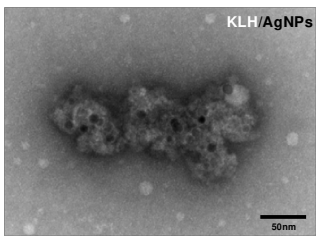

Figure-1

Figure-1. Nanoparticle characterization.

A) Table summarizing the main characteristics of NPs used in the studied as provided by NanoComposix company, n.r = not reported for this batch. Assuming that 1 EU=0.2 ng, nanoparticles used in the studied presented less than 1pg of endotoxin per µg of AgNPs or 0.5pg per µg of AuNPs. B) Absence of AgNPs aggregation was confirmed by TEM as described in M&M section. C) Alveolar macrophages (MPI cell line) or bone marrow derived dendritic cells (BMDC) were incubated with either LPS (100ng/ml) or AgNPs (5µg/ml) and 24h later cytokines were measured in the supernatants by commercial sandwich ELISA. D) KLH (50µg) was mixed with AgNPs (25µg) in a final volume of 50µl. 2µl of 1/50 dilution was analysed by TEM after negative coloration as described in M&M section.

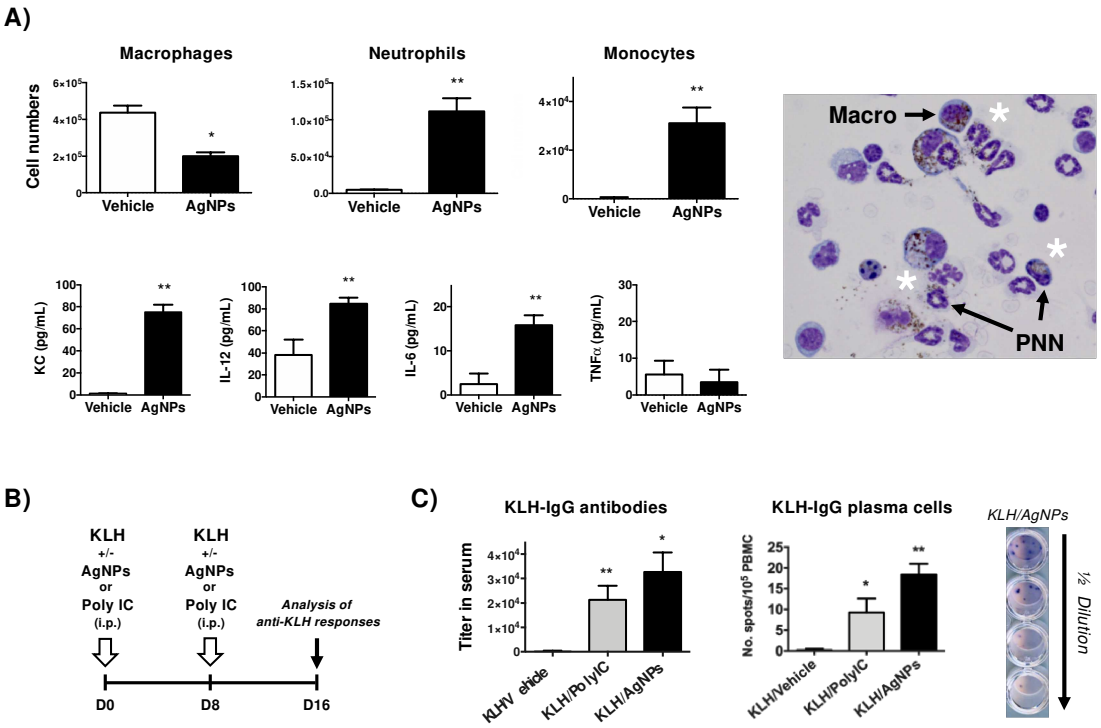
A)
Macrophages
Neutrophils
Monocytes
Cell numbers
Vehicle
AgNPs
Macro
PNN
KC (pg/mL)
IL-12 (pg/mL)
IL-6 (pg/mL)
TNFα (pg/mL)
B)
KLH
+/-
AgNPs
or
Poly IC
(i.p.)
Analysis of
anti-KLH responses
D0
D8
D16
C)
KLH-IgG antibodies
KLH-IgG plasma cells
Titer in serum
No. spots/10^5 PBMC
KLH/Vehicle
KLH/PolyIC
KLH/AgNPs
KLH/AgNPs
½ Dilution

Figure-2

Figure-2. Silver nanoparticles exert proinflammatory activity and enhance specific immunity against KLH protein during intraperitoneal immunization.

A)C57Bl/6 mice were treated with AgNPs (2mg/Kg) intraperitoneally (i.p) and 4h later cells were recovered from peritoneal lavages (10ml) and analysed by flow cytometry and differential coloration in cytospin samples (40x magnification). Macro=macrophage; PNN=polynuclear neutrophil. Asterisks indicate cells that have internalized AgNPs. Peritoneal macrophages, neutrophils and monocytes were also identified as $CD11b^{+}F4/80^{+}$, $CD11b^{+}LyG^{+}Ly6C^{dim}$ and $CD11b^{+}LyG^{-}Ly6C^{high}$, respectively, by flow cytometry and cytokine protein levels were measured with commercial sandwich ELISAs. B) and C) C57Bl/6 mice were immunized i.p with KLH (50µg/mice) mixed with either AgNPs (2mg/Kg) or Poly IC (50 µg/mice) following the experimental protocol described in B). A boost was performed with half doses of KLH, AgNPs and Poly IC. C) At day 16, serum KLH-IgG titers were obtained after ELISA dosage of specific antibodies. Spleen-derived peripheral blood mononuclear cells (PBMC) were used to identify KLH-IgG secreting plasma cells by ELISPOT (see histogram quantification and photograph) *p<0.05, **p<0.01 *vrs*. Vehicle (A), Mann-Whitney test; *vrs* KLH/vehicle (C), Kruskal-Wallis test, (n=3-5 mice per group).

A)

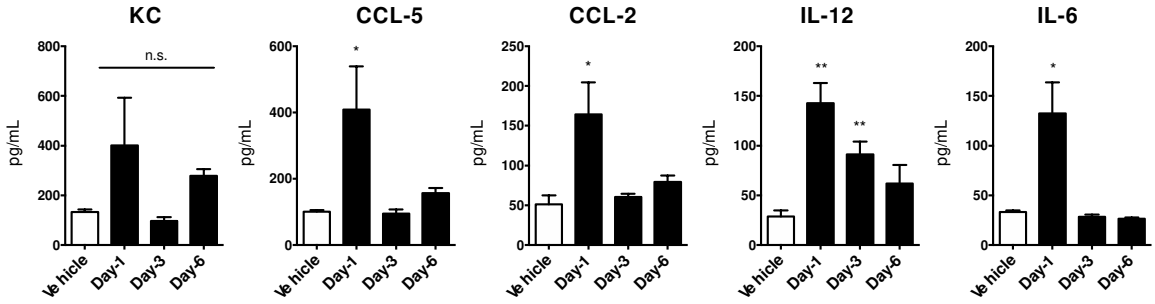
KC
CCL-5
CCL-2
IL-12
IL-6
pg/mL
n.s.
*
**
Vehicle
Day-1
Day-3
Day-6

B)

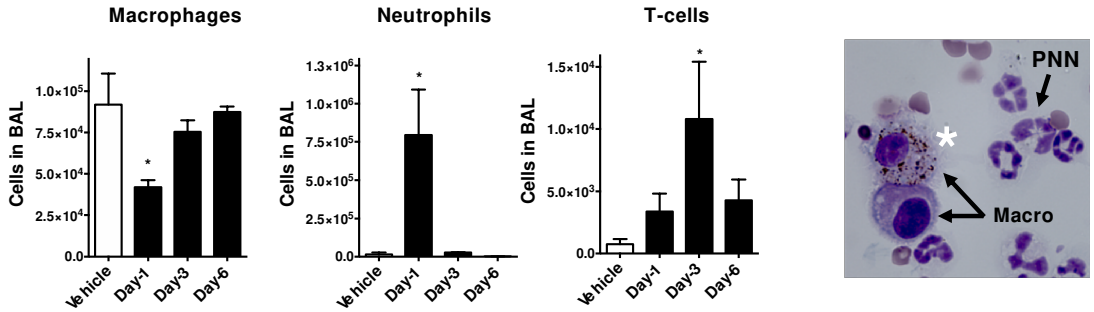
Macrophages
Neutrophils
T-cells
Cells in BAL
*
Vehicle
Day-1
Day-3
Day-6
PNN
Macro

Figure-3

Figure-3. Delivery of silver nanoparticles through the pulmonary route induces transitory local inflammation.

C57Bl/6 mice were intratracheally instilled (i.t) with AgNPs (1mg/Kg) and BALs (2mls) were recovered at either day-1 (D1), D3 or D6 post-treatment. A) Cytokines levels were measured in cell-free (centrifuged) BALs by commercial sandwich ELISA. B) Alveolar macrophages ($CD11c^{+}CD11b^{-/low}SiglecF^{+}$), neutrophils ($CD11b^{+}LyG^{+}Ly6C^{dim}$) and T-cells ($CD3^{+}$) were identified by flow cytometry. The photograph shows a representative BAL cytospin from a mouse treated for 24h with AgNPs. Alveolar macrophages (Macro) are able to engulf instilled AgNPs (white asterisk). *$p<0.05$, **$p<0.01$ *vrs*. Vehicle; Kruskal-Wallis test (n=3-5 mice per group).

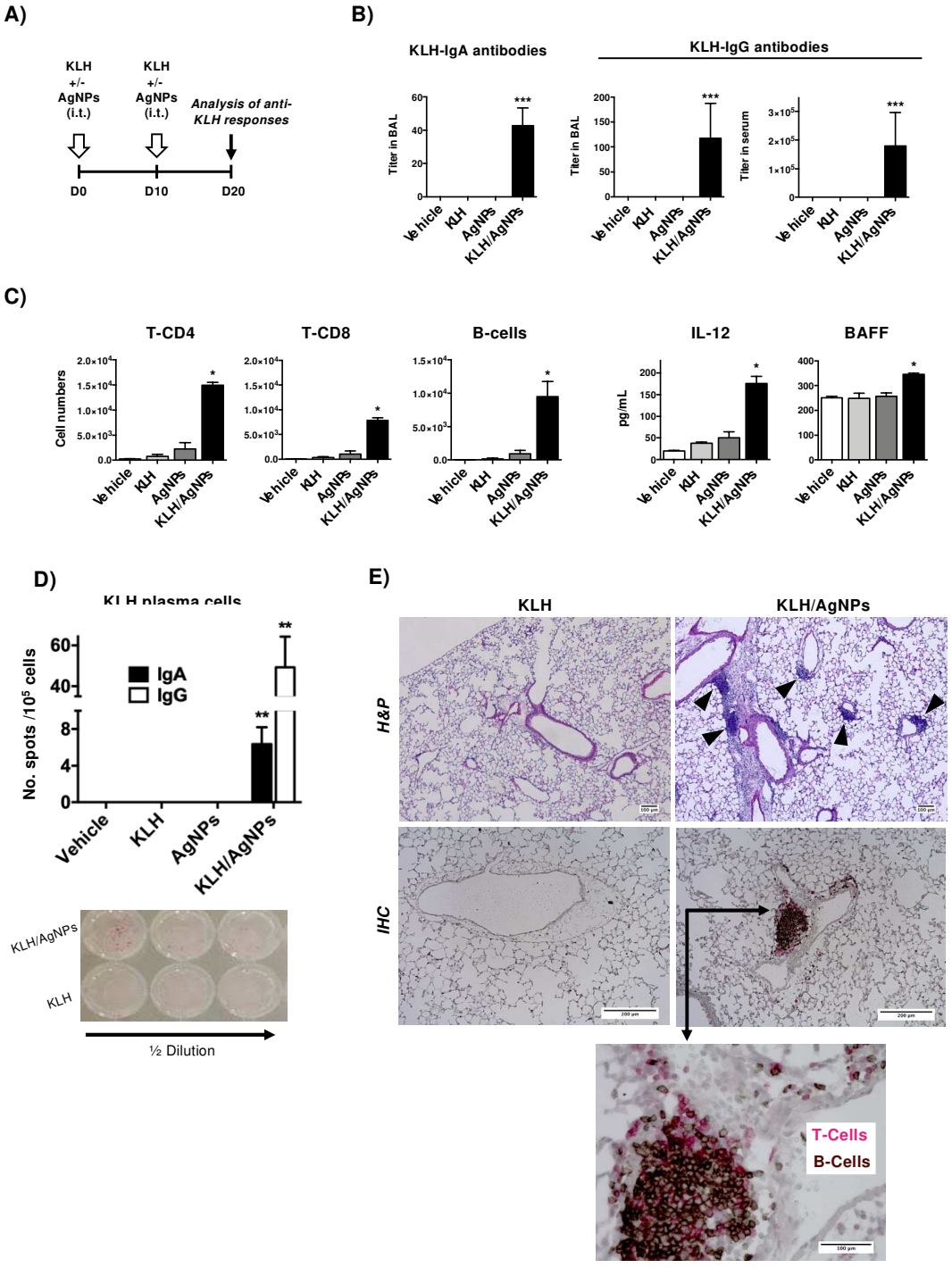
A)
KLH +/- AgNPs (i.t.)
KLH +/- AgNPs (i.t.)
Analysis of anti-KLH responses
D0
D10
D20
B)
KLH-IgA antibodies
KLH-IgG antibodies
Titer in BAL
Titer in serum
***
Ve hicle
KLH
AgNPs
KLH/AgNPs
C)
T-CD4
T-CD8
B-cells
IL-12
BAFF
Cell numbers
pg/mL
*
D)
KLH plasma cells
No. spots /10^5 cells
IgA
IgG
**
Vehicle
KLH
AgNPs
KLH/AgNPs
KLH/AgNPs
KLH
½ Dilution
E)
KLH
KLH/AgNPs
H&P
IHC
T-Cells
B-Cells

Figure-4

Figure-4. Silver nanoparticles enhance mucosal specific immunity against KLH through organization of B/T cell aggregates

A)Protocol of pulmonary immunization. C57Bl/6 mice were i.t instilled with either Vehicle, KLH (50µg/mice), AgNPs (1mg/Kg) or a mixture of KLH/AgNPs at D0. 10 days later (D10), mice were treated under the same conditions with half-dose of reagents (boost). 10 days after the boost (D20), mice were sacrificed and BALs and lungs were collected. B) D20 titers of KLH specific IgA and IgG antibodies in the BALs and serum of immunized mice. C) D20 BAL cellular recruitment in immunized mice. T-cells ($CD3^+CD4^+$ and $CD3^+CD8^+$) and B-cells ($B220^+CD19^+$) were identified by flow cytometry. D) KLH-IgG and KLH-IgA secreting plasma cells in the para-tracheal lymph nodes of immunized mice (D20) were identified by ELISPOT. E) Perfused lungs of immunized mice (D20) were fixed and included in paraffin. Hematoxylin/Phloxin staining (*H&P*) was performed to identify cellular infiltrates in lung parenchyma (black short arrows). Lower panels (*IHC*), antibodies against CD3 and B220 were used to identify in the same slice T-cells (red) and B-cells (brown), respectively, as indicated in Materials and Methods section. Representative images from KLH and KLH/AgNPs immunized mice are shown (from 3-5 mice analysed by group). Mice from Vehicle- or AgNPs-treated groups did not present cellular aggregates (not shown). In B, C and D, *$p<0.05$, **$p<0.01$, ***$p<0.001$ *vrs*. KLH, Kruskal-Wallis test (n=3-5 mice per group).

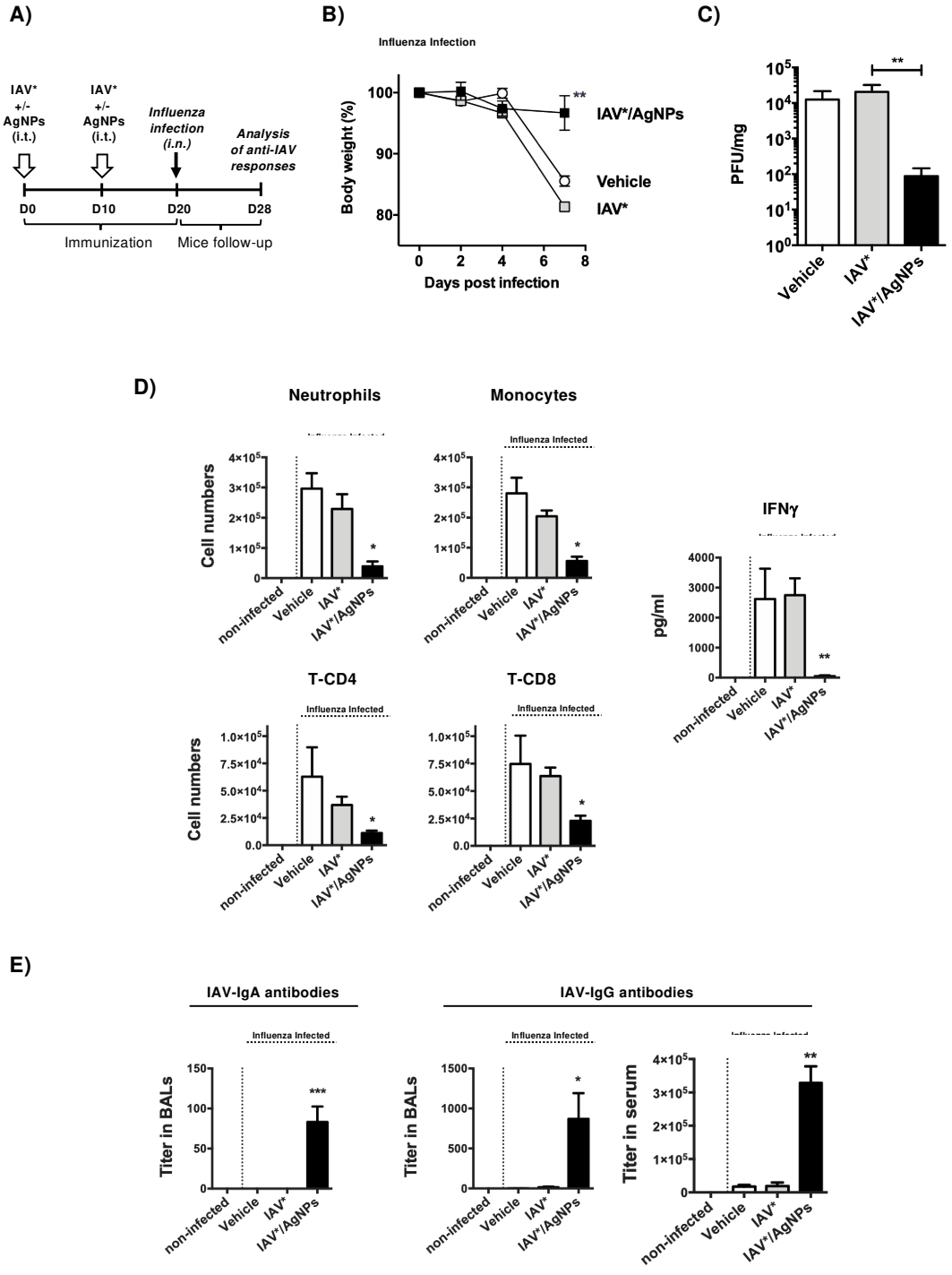
A)
IAV*
+/-
AgNPs
(i.t.)
IAV*
+/-
AgNPs
(i.t.)
Influenza
infection
(i.n.)
Analysis
of anti-IAV
responses
D0
D10
D20
D28
Immunization
Mice follow-up
B)
Influenza Infection
Body weight (%)
Days post infection
IAV*/AgNPs
Vehicle
IAV*
C)
PFU/mg
Vehicle
IAV*
IAV*/AgNPs
D)
Neutrophils
Monocytes
Cell numbers
Influenza Infected
non-infected
Vehicle
IAV*
IAV*/AgNPs
IFNγ
pg/ml
T-CD4
T-CD8
E)
IAV-IgA antibodies
IAV-IgG antibodies
Titer in BALs
Titer in serum

Figure-5

Figure-5. Pulmonary immunization with heat-killed influenza virus in the presence of silver nanoparticles protects mice against sublethal flu.

A) C57Bl/6 mice were i.t immunized at D0 with either Vehicle, heat-killed influenza virus (IAV*) (12μg/mice) or a mixture of IAV*/AgNPs (1mg/Kg). 10 days later (D10), mice were treated under the same conditions with half-dose of reagents (boost). 10 days after the boost (D20), mice were intranasally (i.n) infected with a sublethal dose of live IAV virus (300pfu). Then, body weight loss (% from the day of infection) was followed until d8pi (days post-infection) (B). At d8pi, viral loads in lung homogenates (pfu per mg of total protein) (C), cellular recruitment and IFN-γ levels (D) and titers of IAV-specific IgA and IgG antibodies (E) were quantified in BALs. Cell phenotypes were characterized by flow cytometry as described in M&M section. IFNγ was measured by sandwich ELISA (D). In B, **p<0.01 *vrs* IAV*, Mann-Whitney test (n=3-5 mice per group). In C, D and E, *p<0.05, **p<0.01, ***p<0.001 *vrs*. IAV*, Kruskal-Wallis test (n=3-5 mice per group).

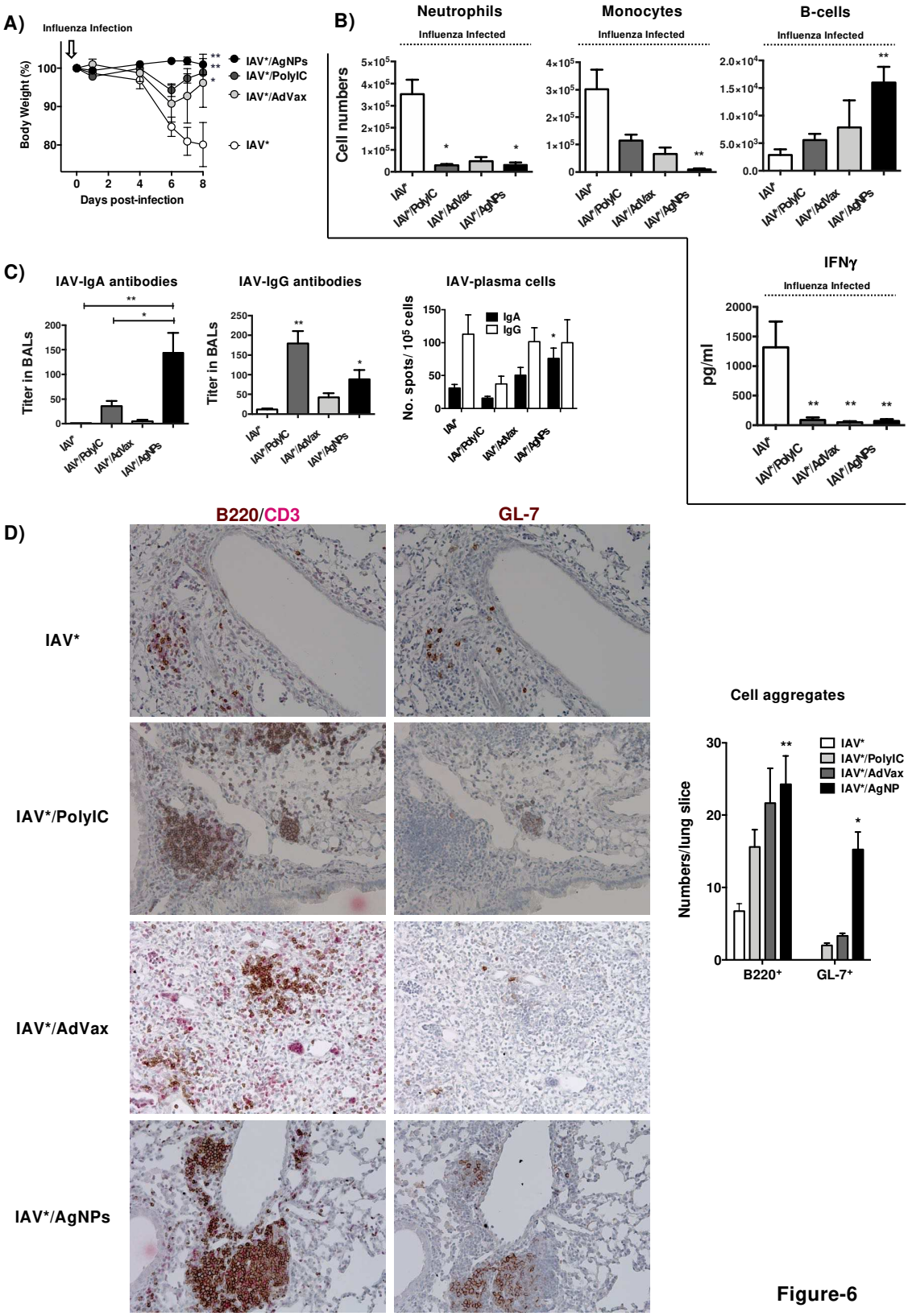
A)
Influenza Infection
Body Weight (%)
Days post-infection
IAV*/AgNPs
IAV*/PolyIC
IAV*/AdVax
IAV*
B)
Neutrophils
Monocytes
B-cells
Influenza Infected
Cell numbers
C)
IAV-IgA antibodies
IAV-IgG antibodies
IAV-plasma cells
Titer in BALs
No. spots/ 10^5 cells
IgA
IgG
IFNγ
pg/ml
D)
B220/CD3
GL-7
IAV*
IAV*/PolyIC
IAV*/AdVax
IAV*/AgNPs
Cell aggregates
Numbers/lung slice
IAV*/AgNP
B220+
GL-7+

Figure-6

Figure-6. Silver nanoparticles preferentially favour local IgA production and germinal centers formation compared to other adjuvants.

Using a similar timing as that depicted in Fig 5, C57Bl/6 mice were first i.t immunized at D0 with IAV* (12µg/mice) alone or combined with either Poly IC (25µg/mice), AddaVax (10µl/mice) or AgNPs (1mg/Kg). A boost was then performed at D10, with a half-dose of reagents, and mice were then infected at D20 with a sublethal dose of live IAV (300pfu), following the protocol depicted in Fig-5A. Body weight loss was followed (A) and at d8pi, cellular recruitment (B), IFN-γ levels (B) and titers of IAV-specific IgA and IgG antibodies (C) were measured in the BALs. In C) right panel, IAV-IgG and IAV-IgA secreting plasma cells were quantified at d8pi in the paratracheal lymph nodes; left and middle panels: IAV-IgA and -IgG were measured in d8pi BALs. In D), sequential lung sections (4 µm) from perfused lungs were stained with anti-CD3 (red)/anti-B220 (brown) antibodies (left panels) or anti-GL-7 antibodies (brown) (right panels) to localize germinal centers (GC) ($GL7^+$) within T/B aggregates. Images were acquired at 20x magnification. In bar charts in D), cell aggregates ($B220^+$ or $GL7^+$) were quantified in different slices considering at least 15 positive cells/aggregate. Different lung sections from 3-5 mice per condition (IAV*/adjuvant mixture) were analysed. In A), *p<0.05, **p<0.01, *vrs*. IAV* Mann-Whitney test. In B), C) and D), *p<0.05, **p<0.01, *vrs*. IAV*, Kruskal-Wallis test (n=3-5 mice per group).

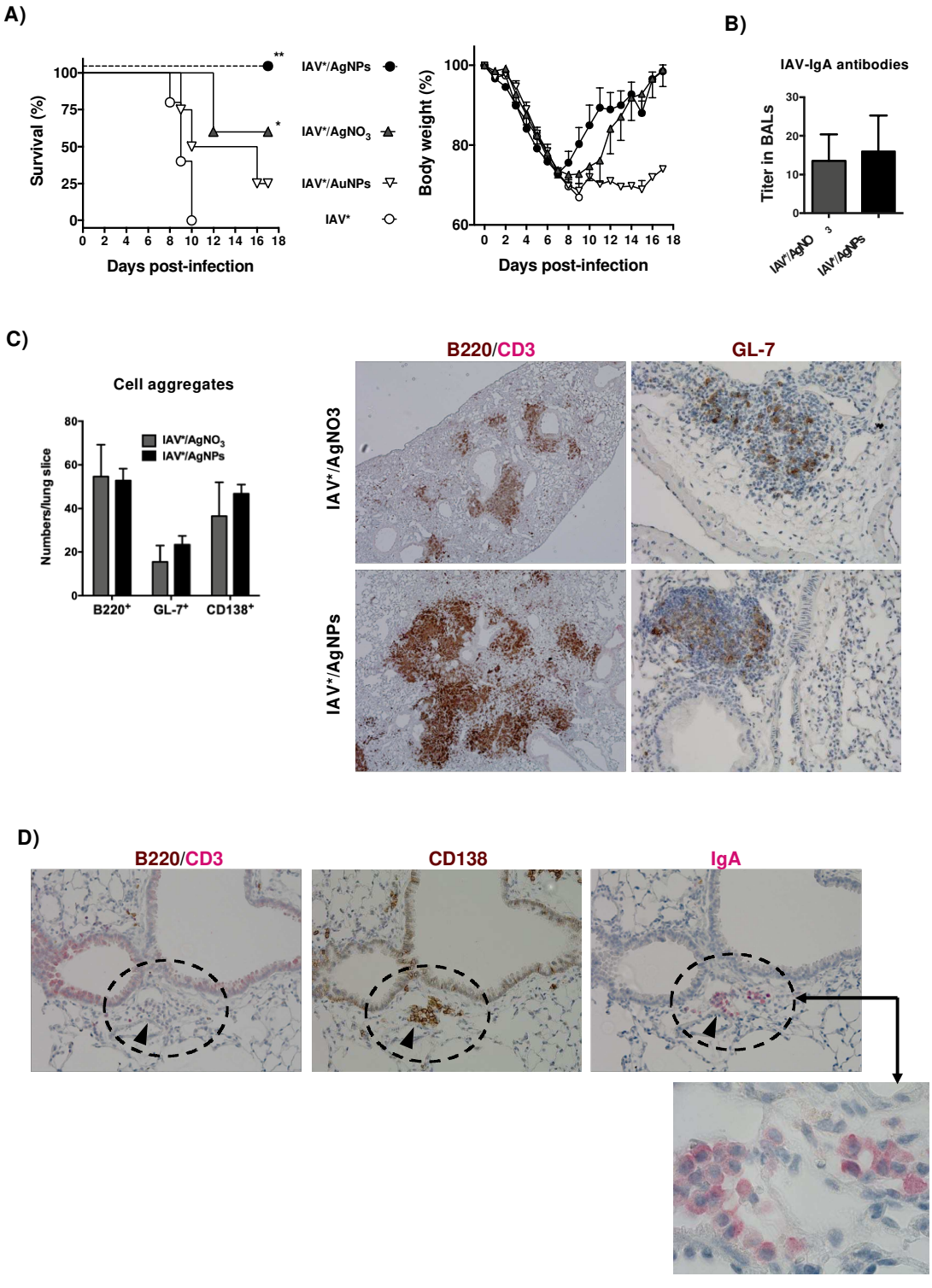
A)
Survival (%)
Days post-infection
IAV*/AgNPs
IAV*/AgNO3
IAV*/AuNPs
IAV*
Body weight (%)
Days post-infection
B)
IAV-IgA antibodies
Titer in BALs
IAV*/AgNO3
IAV*/AgNPs
C)
Cell aggregates
Numbers/lung slice
IAV*/AgNO3
IAV*/AgNPs
B220+
GL-7+
CD138+
B220/CD3
GL-7
IAV*/AgNO3
IAV*/AgNPs
D)
B220/CD3
CD138
IgA

Figure-7

Figure-7. Vaccination with silver nanoparticles or silver salts protects mice from lethal flu.

At D0, C57Bl/6 mice were i.t immunized with either IAV* (12µg/mice) alone or with combinations of either IAV*/gold nanoparticles (AuNPs), IAV*/$AgNO_3$ or IAV*/AgNPs (all at a concentration of 1mg/Kg). A boost was then performed at D10 with half-dose of reagents and mice were finally infected with a lethal dose of IAV (1000 pfu) following the protocol depicted in Fig-5A. A) Body weight loss (% from the day of infection) and survival curves were monitored for each condition. At d18pi, BALs of surviving mice were analysed for IAV-specific IgA antibodies (B), and lungs parenchyma were monitored for the presence of aggregates of T/B cell (B220/CD3, 5x magnification, C), GC ($GL\text{-}7^+$, 20x magnification, C) and $CD138^+$ (more than 15 positive cells/aggregate), as described in Fig-6. Different lung sections were analysed from 3-5 mice per condition. In D), sequential slides (4µm) of lungs from IAV*/AgNPs vaccinated mice were stained with anti-B220/CD3, anti-CD138 or anti-IgA antibodies. Images were acquired at either 20x or 100x magnification, to demonstrate specific IgA staining. In A) *$p<0.05$, **$p<0.01$ Log-Rank (Mantel-Cox) test (n=5 mice per group).

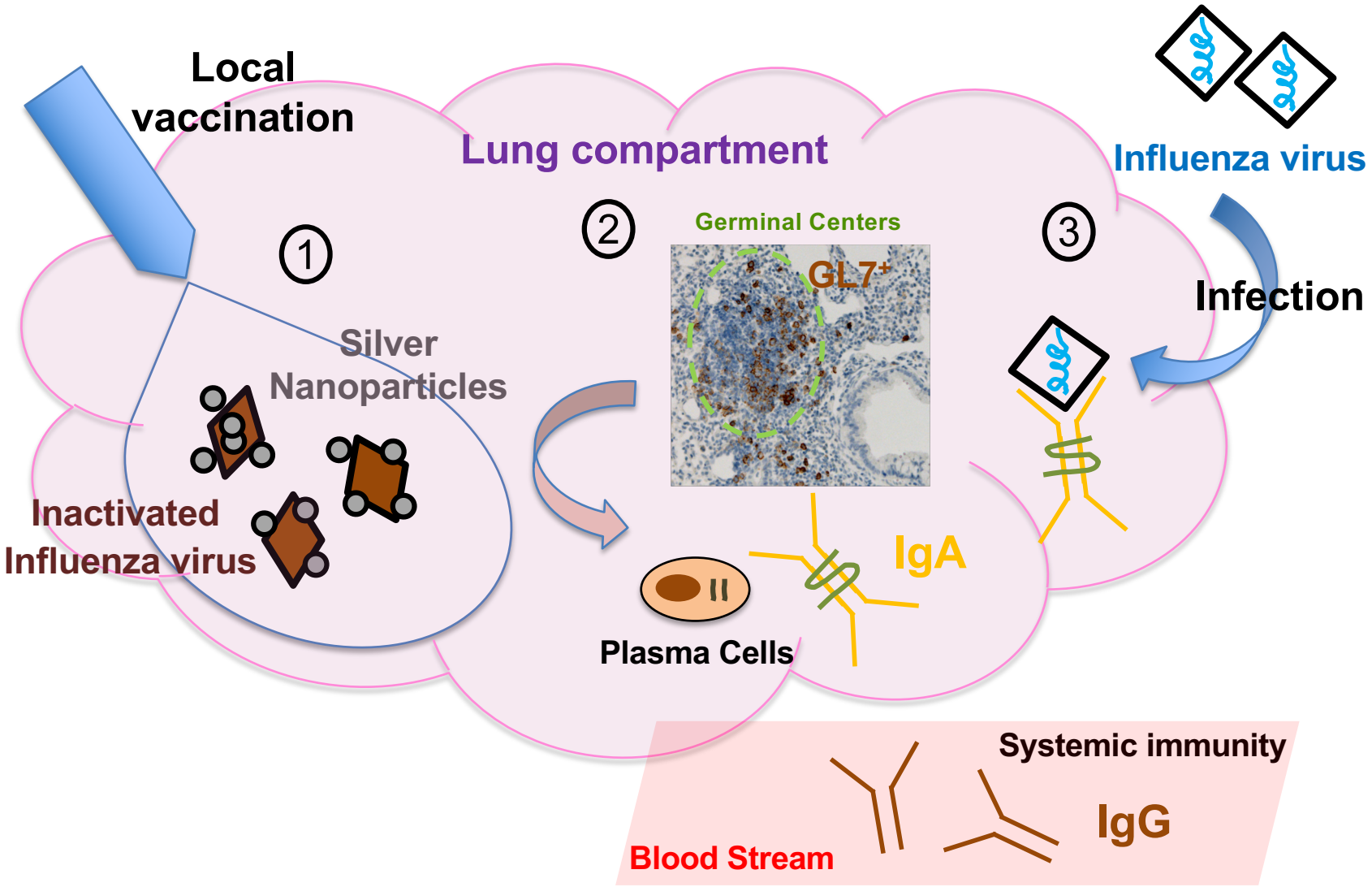

Graphical Abstract. Vaccination with inactivated influenza virus using silver nanoparticles as adjuvant through the respiratory route (**1**), promotes local and systemic immunity against influenza virus (anti-Influenza IgA and IgG antibodies) (**2**) and favours bronchus-associated lymphoid tissue (BALT) neogenesis (**2**), which in turns protects against further influenza infection (**3**). Vaccination only with the antigen (inactivated virus) does not confer protection against viral challenge.